Available online at www.sciencedirect.com

SciVerse ScienceDirect

Ceramics International 39 (2013) 829–833

CERAMICS INTERNATIONAL

www.elsevier.com/locate/ceramint

Effect of annealing atmosphere on the epitaxial growth process of $La_2Zr_2O_7$ films on different substrates

Y. Wang*, Y.F. Lu, L. Zhou, C.S. Li, Z.M. Yu, J.Q. Feng, L.H. Jin, P.F. Wang, H. Wang

Northwest Institute for Nonferrous Metal Research, Xi'an 710016, PR China

Received 18 April 2012; received in revised form 29 June 2012; accepted 1 July 2012
Available online 8 July 2012

Abstract

We have studied the effect of annealing atmosphere on the epitaxial growth process of $La_2Zr_2O_7$ (LZO) thin films on different substrates fabricated by metal-organic deposition (MOD) method. The structure, texture and morphology of LZO films were investigated by X-ray diffraction (XRD) and atomic force microscopy (AFM). Our results show that the epitaxial growth process of LZO thin film does not completely depend on the lattice mismatch degree between LZO and substrate, and it may be related to the oxygen vacancy defects and the lattice ordering degree. Moreover, the decrease of the lattice oxygen vacancy defects may be beneficial to suppressing the stress and strain relaxation within epitaxial film. The grain boundary concentration in epitaxial films is also related to their strain relaxation process. These results are significant not only to improving the performance of coated conductors, but also to developing other epitaxial oxide thin film on textured substrate.

Keywords: Coated conductors; Buffer layer; Metal-organic deposition; Epitaxial growth

1. Introduction

For second generation high-temperature superconducting coated conductors consisted of metallic substrate/buffer layer/superconducting layer/protective layer, buffer layer is a key functional layer [1–3]. A key issue in preparation process of high-performance coated conductors is the necessity to obtain buffer layer with perfect bi-axial texture that induces the orientation growth of superconducting layer. During the last few years, lot of effort has been made to study the factors influencing the texture growth of buffer layer in coated conductors. In the Rolling-assisted bi-axially textured substrates (RABiTS) route, epitaxial growth of buffer layer on textured metallic substrate is very important to realize the bi-axial texture of superconducting layer. Therefore, the investigation of the factors influencing epitaxial growth of buffer layer is significant not only to improving the performance of coated conductors, but also to developing other epitaxial oxide thin film on textured substrate.

$La_2Zr_2O_7$ (LZO) with pyrochlore structure appears to display low oxygen diffusivity and high structural and chemical compatibility with NiW and YBCO. Although the lattice mismatch between LZO and NiW is much higher, LZO thin film is still allowed good epitaxial growth on textured NiW substrate [4,5]. A tilting mechanism is believed to play an important for strain relief in this highly strained system of LZO with respect to NiW (compressive) [6]. The preparation procedures for LZO thin films on single crystal substrates and textured NiW tapes by metal-organic deposition (MOD) method are readily controllable and rather mature [7–10]. Moreover, upon high-temperature or high-pressure situation, pyrochlore LZO easily changes to a defect fluorite structure because of the cation antisite defects formation energy [11]. Therefore, we choose LZO as a model buffer material and prepare LZO thin films with pyrochlore structure on single crystal substrates with different lattice mismatch in reducing and oxidation annealing atmosphere by MOD method.

*Corresponding author.
E-mail address: wyspacestar@yahoo.com.cn (Y. Wang).

0272-8842/$36.00 © 2012 Elsevier Ltd and Techna Group S.r.l. All rights reserved.
http://dx.doi.org/10.1016/j.ceramint.2012.07.004

Afterward, the effect of annealing atmosphere on the epitaxial growth process of LZO thin films on different substrates is explored by investigating texture and morphology evolution of LZO films on different substrates fabricated in different annealing atmosphere.

2. Experimental procedure

The CSD precursor solution was prepared in ambient atmosphere. The reagents Lanthanum (III) 2,4- and Zirconium (IV) 2,4-pentanedionate were used as received from Strem. Stoichiometric quantities of Lanthanum 2,4-pentanedionate and Zirconium 2,4-pentanedionate were dissolved in propionic acid and heated at 75 °C with continuous stirring to obtain a stable yellow-colored LZO precursor solution with 0.3 M total cation concentration. Details of the preparation process can be founded elsewhere [7–10]. This solution was then spin-coated onto YSZ (*l*00), LAO (*l*00) and STO (*l*00) single crystal substrates at 2500 rpm for 30 s, respectively. The coating samples were heated treatment at 900 °C for 1 h in a reducing forming gas atmosphere of Ar-4%H_2 and air afterwards, respectively. The samples were finally quenched to room temperature with the same atmosphere.

The LZO films on the different single crystal substrates were characterized by X-ray diffraction (XRD), which was performed to carry out θ–2θ scan using CuKα radiation at 40 kV and 50 mA, for phase purity and texture. The lattice parameters were determined from XRD patterns using the MDI-JADE-6 program. The film thickness of LZO were calibrated and determined by α-step apparatus. The microstructure and surface roughness of as-grown samples were performed by a digital instruments nanoscope SRI3800-SPA-400 atomic force microscopy (AFM) in contact mode.

3. Results and discussion

XRD θ–2θ spectrum for LZO films, whose thickness calibrated by α-step apparatus are nearly 20 nm, deposited on YSZ, LAO and STO single crystal substrates in Ar-4%H_2 atmosphere are shown in Fig. 1. From the XRD patterns, it was found that all the LZO films on single crystal substrates with different lattice mismatch degree have completely crystallized to form a preferred orientation along the (*l*00) direction. It should be pointed out that there is a clear division of LZO (400) peak epitaxially grown on LAO substrate. It may result from partially relaxed stress within the LZO film with the increase of LZO thickness. In other words, the partially relaxed stress within the LZO film disturbed the surface layer of LZO film, while the interface layer of LZO film is still the complete strained film.

Fig. 2 shows XRD relative intensity of LZO (400) peak in the samples fabricated in Ar-4%H_2 (determined by taking the intensity ratio of LZO (400) to the strongest peaks of substrates) and FWHM of LZO (400) peak as a function of the lattice mismatch degree between substrate and LZO. The lattice mismatch degree f between substrate and epitaxial film can be calculated by Eq. (1) [12].

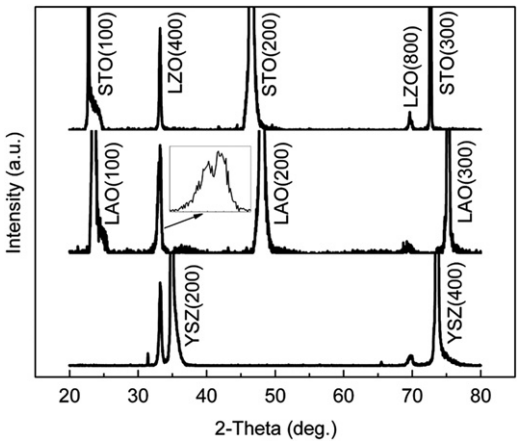

Fig. 1. Typical θ–2θ scans for LZO films grown on (a) YSZ, (b) LAO and (c) STO single crystal substrates in Ar-4%H_2.

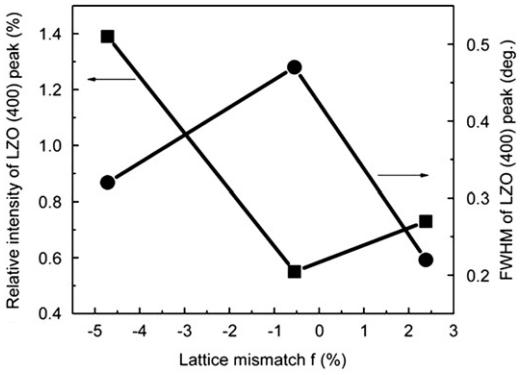

Fig. 2. The relative intensity of LZO (400) peaks and their FWHM values for LZO films obtained in Ar-4%H_2 as a function of lattice mismatch degree between substrate and LZO.

$$f = \frac{\alpha_s - \alpha_e}{\alpha_e}. \quad (1)$$

where α_s is the lattice parameter of substrate, and α_e is the intrinsic lattice parameter of epitaxial film. The lattice mismatch degree between YSZ, LAO, STO and LZO is −4.72%, −0.55% and 2.38%, respectively.

The relative intensity of LZO (400) peak of LZO film deposited on LAO substrate is the weakest in all the samples prepared in the same conditions, which may be related to the division of LZO (400) diffraction peak on LAO substrate. However, the relative intensity of LZO (400) peak of LZO film on YSZ single crystal substrate is larger than that on STO substrate. It illuminates that the epitaxial growth of LZO thin film does not completely depend on the lattice mismatch degree between LZO and substrate, and it may be related to the oxygen vacancy defects and the lattice ordering degree [11]. In fact, the epitaxial growth of oxide film could be still realized under certain conditions of the large lattice mismatch between epitaxial film and substrate [13–15].

The size of crystal grain was estimated using Scherrer's Eq. (2) [16,17],

$$D = \frac{\kappa\lambda}{B\cos\theta}. \quad (2)$$

where D is the particle diameter, λ denotes the X-ray wavelength, B is the full-width at half-maximum (FWHM) of the X-ray diffraction peak, θ is the diffraction angle, and k is the Scherrer constant of the order of unity for usual crystals. From Fig. 2, it can be seen that the FWHM values of LZO (400) diffraction peaks of LZO films deposited respectively on LAO, YSZ and STO substrates decrease in sequence, which suggests that their crystallization degree and the size of crystal grains increase in sequence. Therefore, it can be considered that the growth speed of LZO grains on the above-mentioned three kinds of substrates increases in sequence, which results in the decrease of the grain boundary concentration in LZO crystallized film in sequence. The increase in FWHM values of XRD peaks in thin films is related to the reduction of particle size, the increase in the grain boundary and enhancement of lattice strain [18–19]. Moreover, it may be associated with the worse orientation of LZO thin film on LAO and STO substrates and the division phenomena of LZO (400) diffraction peak on LAO substrate.

The typical XRD θ–2θ scan results of the as-grown LZO thin films on YSZ, LAO and STO substrates obtained in air are shown in Fig. 3. All the LZO films deposited on these single crystal substrates prepared in air have completely crystallized to form the preferred orientation along the (l00) direction. It should be pointed out that the division phenomena of LZO (400) peak does not be observed in the sample of LZO film deposited on LAO substrate in air. It illustrates that the LZO film fabricated on LAO substrate in air may be a complete strained film. The epitaxial growth mechanism of LZO film on the same substrate is not the same one in different heat-treatment atmosphere. Moreover, the decrease of the lattice oxygen vacancy defects may be beneficial to suppressing the stress and strain relaxation. For the LZO films fabricated in air, their thickness is almost the same as that prepared in Ar-4%H_2, in other words, the difference between the thickness of LZO films prepared in air and that fabricated in Ar-4%H_2 could be ignored at the present test technique due to the limited precision.

Fig. 4 illustrates the relative intensity and FWHM values of the LZO (400) diffraction peak as a function of the lattice mismatch degree between LZO and substrate. It reveals that the relative intensity of LZO (400) peak of LZO film on LAO substrate is the largest in the same preparation condition, which suggests that LZO film deposited on LAO substrate with smallest lattice mismatch shows the best (l00) orientation. It is likely that texture of LZO films on STO and YSZ substrates fabricated in air get bad due to the growing population of lattice defects as a result of the lattice mismatch [20]. In addition, the FWHM values of LZO (400) diffraction peaks of LZO films on YSZ, LAO and STO substrates decrease in sequence. It indicates that the growth speed of LZO grains on the

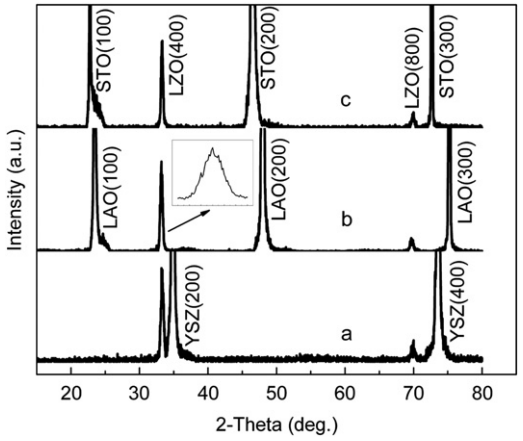

Fig. 3. XRD patterns for LZO films on (a) YSZ, (b) LAO and (c) STO single crystal substrates annealed in air.

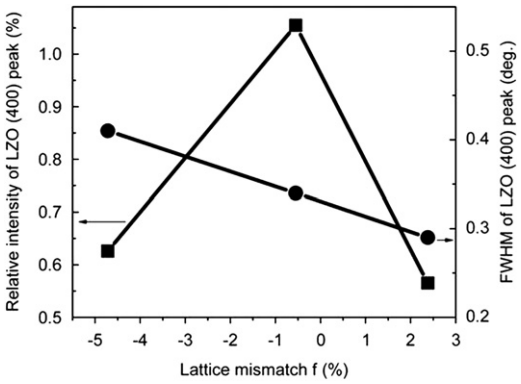

Fig. 4. Dependence of the relative intensity and FWHM values of LZO (400) diffraction peaks for LZO film on (a) YSZ, (b) LAO and (c) STO single crystal substrates prepared in air.

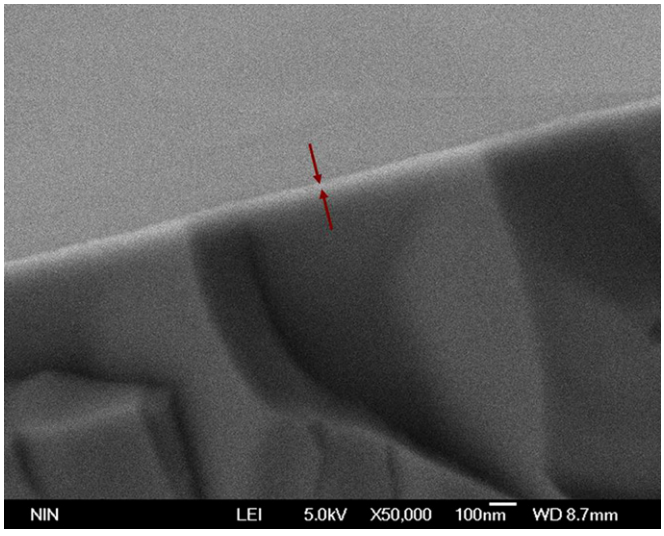

Fig. 5. An x-section image on the LZO film on YSZ substrate deposited in air.

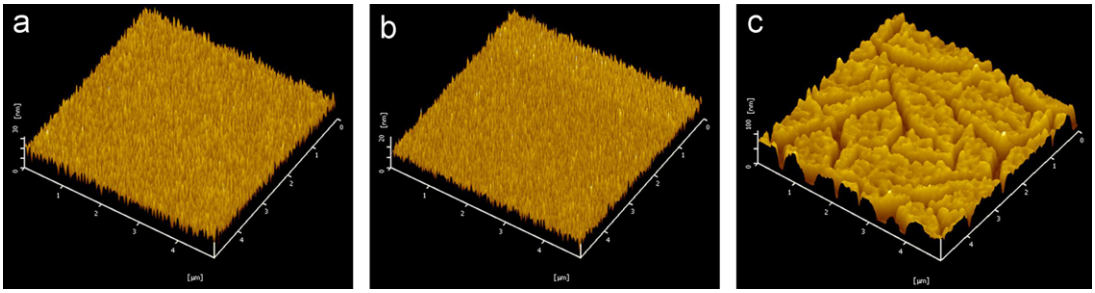

Fig. 6. AFM images for LZO films on (a) YSZ, (b) LAO and (c) STO single crystal substrates fabricated in Ar-4%H_2.

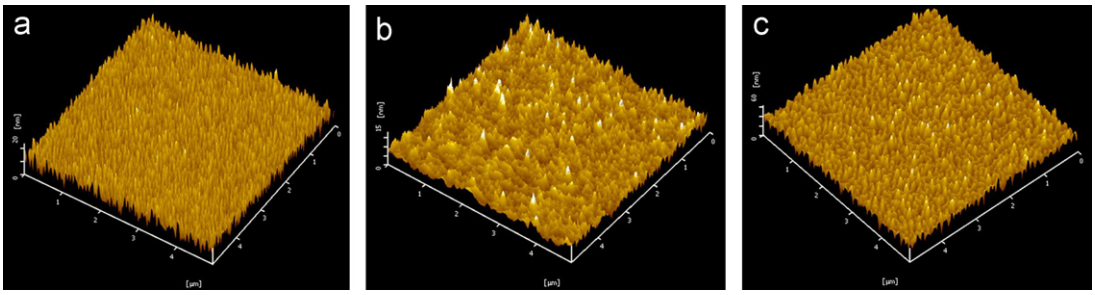

Fig. 7. AFM micrograph of LZO films on (a) YSZ, (b) LAO and (c) STO single crystal substrates prepared in air, respectively.

above-mentioned three kinds of substrates increase at the same preparation conditions in sequence, which leads to the decrease of the grain boundary concentration of LZO film in sequence. These results may be related to worst orientation of LZO film deposited on STO substrate.

A cross-section image on the LZO film on YSZ substrate deposited in air is shown in Fig. 5 and a sharp interface of the LZO film and YSZ substrate could be seen. The LZO film appears homogeneous in thickness and without obvious macroscopic defects. The thickness of LZO film was determined to be about 20 nm.

Figs. 6 and 7 show AFM images for LZO films with the same thickness on different single crystal substrates annealed in Ar-4%H_2 and air. Dense, crack-free and homogenous surface morphologies are observed in all samples except the LZO film on STO substrate prepared in Ar-4%H_2. Surface roughness increase according to the sequence of LZO films on LAO, YSZ and STO substrates, typical values observed increase from 3.08–3.80 and finally to 18.45 nm at an annealing atmosphere of Ar-4%H_2, while the roughness values increase from 1.66–3.43 and finally to 7.31 nm for the samples prepared in air. Average grain size of LZO films on STO substrates are the biggest whether fabricated in Ar-4%H_2 or air. For the samples annealed in Ar-4%H_2, the average grain size of LZO film on YSZ substrate is bigger than that on LAO substrate, but the results obtained in air is just in opposition. It is noted that the grain boundary concentration within epitaxial film increase as the decrease of average grain size of film. In any case the surface roughness values of LZO film on LAO substrate with smallest lattice mismatch degree is the smallest in all samples whether annealed in reducing or oxidation atmosphere.

According to above analysis, the lattice mismatch degree with LZO film is the largest for YSZ substrate, while it is smallest for LAO substrate. We have clearly seen that the LZO film on YSZ substrate shows a better c-axial orientation than that on LAO substrates annealed in Ar-4%H_2. Hence a dependence of epitaxial growth of LZO films on the lattice mismatch degree between LZO and substrates is not confirmed. However, relative intensity and FWHM change of LZO (400) diffraction peaks is very different in the samples annealed in Ar-4%H_2 and air, which may be due to some changes of growth mechanism in different annealing atmosphere [21]. In addition, the lattice ordering degree of LZO may be destroyed in the high-temperature annealing process. It suggests that both the oxygen vacancies concentration and lattice ordering degree are the important factors to the epitaxial growth of LZO films. For the heteroepitaxial system, the stress and strain in epitaxial film would change as the variation of the lattice mismatch between epitaxial film and substrate. When the stain energy in epitaxial film increases to a certain value, the formation of misfit dislocation would lead to the decrease of the whole system energy and the strain relaxation in epitaxial film would results in the quality decrease of epitaxial film. It can be considered that many factors including the oxygen vacancy concentration and grain boundary concentration in epitaxial film are related to the process of its strain relaxation.

4. Conclusion

In summary, we have successfully fabricated LZO thin films with preferred *c*-axial orientation on YSZ, LAO and STO single crystal substrates by MOD method in annealing atmosphere of Ar-4%H_2 and air, respectively. The effect of annealing atmosphere on the epitaxial growth process of LZO films on different substrates has been studied. The results showed that the lattice mismatch degree between substrate and LZO, the oxygen vacancy defects and lattice ordering degree have significant influence on the epitaxial growth of LZO thin films on textured substrates. The decrease of the lattice oxygen vacancy defects may be beneficial to suppressing the stress and strain relaxation within epitaxial film. Moreover, the grain boundary concentration in epitaxial films is also related to its strain relaxation process.

Acknowledgments

This work was financially supported by the International Science & Technology Cooperation Program of China, National Science Fund Program and National 863 Program of China (Grant Nos. 2012DFA50780, 50872115 and 2008AA03Z202).

References

[1] L. Arda, S. Ataoglu, S. Sezer, Z. Abdulaliyev, Residual stress analysis of multi-layered buffer layers on Ni substrate for YBCO coated conductor, Surface and Coatings Technology 202 (2007) 439–446.

[2] P. Mele, K. Matsumoto, T. Horide, A. Ichinose, M. Mukaida, Y. Yoshida, S. Horii, Enhanced high-field performance in PLD films fabricated by ablation of YSZ-added $YBa_2Cu_3O_{7-x}$ target, Superconductor Science and Technology 20 (2007) 244–250.

[3] Y.-K. Kima, J. Yoo, K. Chung, X. Wang, S.X. Dou, Metal-organic deposition of biaxially textured CeO_2–based buffer layers, Materials Letters 63 (2009) 800–802.

[4] L. Molina, K. Knoth, S. Engel, B. Holzapfel, O. Eibl, Chemically deposited $La_2Zr_2O_7$ buffer layers for YBCO-coated conductors: film growth and microstructure, Superconductor Science and Technology 19 (2006) 1200–1208.

[5] C. Jiménez, T. Caroff, L. Rapenne, S. Morlens, E. Santos, P. Odier, F. Weiss, Effect of the annealing process on the microstructure of $La_2Zr_2O_7$ thin layers epitaxially grown on $LaAlO_3$ by metalorganic decomposition, Journal of Crystal Growth 311 (2009) 3204–3210.

[6] L. Molina, K. Knoth, S. Engel, B. Holzapfel, O. Eibl, Chemically deposited $La_2Zr_2O_7$ buffer layers for YBCO-coated conductors: film growth and microstructure, Superconductor Science and Technology 19 (2006) 1200–1208.

[7] K. Knoth, R. Hühne, S. Oswald, L. Schultz, B. Holzapfel, Detailed investigations on $La_2Zr_2O_7$ buffer layers for YBCO-coated conductors prepared by chemical solution deposition, Acta Materialia 55 (2007) 517–529.

[8] T. Caroff, S. Morlens, A. Abrutis, M. Decroux, P. Chaudouët, L. Porcar, Z. Saltyte, C. Jiménez, P. Odier, F. Weiss, $La_2Zr_2O_7$ single buffer layer for YBCO RABiTS coated conductors, Superconductor Science and Technology 21 (2008) 075007.

[9] S. Engel, R. Hühne, K. Knoth, A. Chopra, N.H. Kumar, V.S. Sarma, P.N. Santhosh, L. Schultz, B. Holzapfel, Optimisation of single $La_2Zr_2O_7$ buffer layers for YBCO coated conductors prepared by chemical solution deposition, Journal of Crystal Growth 310 (2008) 4295–4300.

[10] K. Knoth, R. Hühne, S. Oswald, L. Molina, O. Eibl, L. Schultz, B. Holzapfel, Growth of thick chemical solution derived pyrochlore $La_2Zr_2O_7$ buffer layers for $YBa_2Cu_3O_{7-x}$ coated conductors, Thin Solid Films 516 (2008) 2099–2108.

[11] F.X. Zhang, M. Lang, Z.X. Liu, R.C. Ewing, Pressure-induced disordering and anomalous lattice expansion in $La_2Zr_2O_7$ pyrochlore, Physical Review Letters 105 (2010) 015503.

[12] Z.Q. Wu, B.Z. Wang, The growth of thin film, Sciencep, Beijing, 2001.

[13] M.P. Paranthaman, M.S. Bhuiyan, S. Sathyamurthy, L. Heatherly, C. Cantoni, A. Goyal, Improved textured $La_2Zr_2O_7$ buffer on La_3TaO_7 seed for all-MOD buffer/YBCO coated conductors, Physica C 468 (2008) 1587–1590.

[14] M.S. Bhuiyan, M. Paranthaman, A. Goyal, L. Heatherly, D.B. Beach, Deposition of rare earth tantalate buffers on textured Ni–W substrates for YBCO coated conductor using chemical solution deposition approach, Journal of Materials Research 21 (2006) 767–773.

[15] Y.X. Zhou, S. Bhuiyan, S. Scruggs, H. Fang, M. Mironova, K. Salama, Strontium titanate buffer layers deposited on rolled Ni substrates with metal organic deposition, Superconductor Science and Technology 16 (2003) 901–906.

[16] A.J.C. Wilson, On variance as a measure of line broadening in diffractometry general theory and small particle size, Proceedings of the Physical Society London 80 (1962) 286–294.

[17] Y. Wang, G.F. Zhang, C.S. Li, G. Yan, Y.F. Lu, Growth and structure of $NdGaO_3$ films prepared by metal-organic deposition, International Journal of Materials Research 101 (2010) 349–352.

[18] Z.W. Wang, Y.S. Zhao, D. Schiferl, C.S. Zha, R.T. Downs, Pressure induced increase of particle size and resulting weakening of elastic stiffness of CeO_2 nanocrystals, Applied Physics Letters 85 (2004) 124–126.

[19] K. Sakuma, O. Michikami, Orientational control of CeO_2 buffer layers on A-plane sapphire substrates for $REBa_2Cu_3O_{7-\delta}$ thin films, Physica C 470 (2010) 1452–1456.

[20] M. Mosiadz, R.I. Tomov, S.C. Hopkins, G. Martin, D. Hardeman, B. Holzapfel, B.A. Glowacki, Inkjet printing of $Ce_{0.8}Gd_{0.2}O_2$ thin flims on Ni-5%W flexible substrates, Journal of Sol–Gel Science and Technology 54 (2010) 154–164.

[21] S.B. Kim, S.I. Yoo, Y. Yamada, The effect of post-annealing process in NdGaO3 new seed layer for LPE, Physica C 392–396 (2003) 951–955.